Synthesis and Evaluation of Trimethylolpropane Triacrylate Crosslinked Superabsorbent Polymers for Conserving Water and Fertilizers

Dhanapal Venkatachalam,[1] Vijayakumar Vediappan,[2] Subramanian Kaliappa gounder[2]

[1]Department of Physical Sciences, Bannari Amman Institute of Technology, Sathyamangalam,
638 401 Erode District, Tamil Nadu, India
[2]Department of Biotechnology, Bannari Amman Institute of Technology, Sathyamangalam, 638 401 Erode District, Tamil Nadu, India
Correspondence to: K. Subramanian (E-mail: drksubramanian@rediffmail.com)

ABSTRACT: A series of superabsorbent polymers (SAP) were synthesized by free radical thermal copolymerization of acrylic acid and *N*-isopropyl acrylamide monomers using trimethylolpropane triacrylate as crosslinker. They were characterized by FT-IR and thermal stability (TGA/DTG), and evaluated for their water and fertilizer uptake and release characteristics under different crosslinker levels, temperature, pressure, and pH. The observed maximum absorption of water by the SAP was 1130 g/g of polymer. The release was modeled which showed a non-Fickian mechanism. The water uptake of SAP was correlated with the average molecular weight between the crosslinks and crosslink density. Analysis of the weight loss data from TG in air revealed a zero order kinetics for the initial degradation step with an activation energy (AE) of 70.8 kJ/mol. The AEs for water uptake and release for thermal degradation were also determined through Arrhenius plots. The results inferred that the synthesized SAP can be exploited for commercial agricultural applications. © 2012 Wiley Periodicals, Inc. J. Appl. Polym. Sci. 129: 1350–1361, 2013

INTRODUCTION

Superabsorbent polymers (SAPs) are loosely crosslinked three-dimensional network hydrophilic polymers. They are capable of imbibing and retaining large quantity of water and aqueous fluids such as urine, blood, electrolyte solution etc. more than thousands times their own dry weight under ambient conditions.[1] These were due to their high hydrophilicity, increased entropy of network during absorption, osmotic pressure based on movable counter-ions, affinity between the polymer electrolyte[1] and water etc. They also possess excellent fluid retention properties under pressure[2,3] as they immobilize the fluid by entrapment rather than by holding it in the structure. Because of the aforementioned features, SAPs are finding extensive applications in drug delivery as carriers,[4–6] agricultural and horticultural fields as soil conditioners,[7–10] disposable diapers,[11] hygienic napkins,[12] cement,[13] effluent treatments for removing heavy metals, and dye,[14,15] disposal of radioactive uranium ions,[16] absorbing oil,[17] coal dewatering,[18] sensors[19] etc. Besides, they are also employed in communication cables, humidity control, artificial snow for winter sports, toys, cosmetics and as an industrial absorbent, and for prevention of moisture ingress into walls and ceilings.[20,21] Application of SAP

in soils greatly reduced irrigation induced soil erosion, soil water seepage, irrigation frequency, and increased the uniformity of furrow water applications.[22–24] Moreover, the fragmented products of SAP were reported to be biodegradable and their products do not harm the farmer friendly microbes present in the soil.[25] Because of the excellent water absorption and retention properties, SAPs are increasingly being used globally in agriculture for controlled release of water and fertilizers to manage the drought and to protect the soil from over loading with synthetic fertilizers, respectively. It is to be noted that due to surface runoff, leaching and vaporization, the utilization efficiency or plant uptake of fertilizer is generally below 50%. Moreover, the loss of feeding nutrients could cause very serious environmental problems such as eutrophication,[26–28] blue baby syndrome, and micronutrient imbalance. Hence, there is an increasing demand and ample scope for these materials in agricultural applications. The water absorption-retention characteristics of SAPs can be fine-tuned by the meticulous choice of monomers and crosslinker etc. during synthesis. The present investigation involved the synthesis of a potential SAP with tremendous swellability using an hitherto unreported combination of monomers/crosslinker, such as acrylic acid (AA),

Table I. Monomer Feed Composition, Average Molecular Weight Between Crosslinks ($\overline{M_c}$) and Crosslink Density (q) of Synthesized SAP

SAP code	S/A mole ratio[a]	NIPAAm (M)	TMPTA (M)	$\overline{M_c}$	q	Water uptake (g/g)
ANT-1	0	0.05	0.05	2118	28	44.12
ANT-2	0.01413	0.05	0.05	536,862	7183	123.02
ANT-3	0.0316	0.05	0.05	979,419	13,104	142.3
ANT-4	0.0562	0.05	0.05	1,506,159	20,152	157.34
ANT-5	0.1778	0.05	0.05	16,368,914	219,011	295.22
ANT-6	0.5623	0.05	0.05	55,669,426	744,839	399.77
ANT-7	1.1778	0.05	0.05	84,010,584	1,124,035	325.72
ANT-8	6.3095	0.05	0.05	32,707,866	437,621	303.8
ANT-9	19.4984	0.05	0.05	14,288,963	191,182	258.26
ANT-10	28.1838	0.05	0.05	17,908,692	239,613	250.38
ANT-11	446.684	0.05	0.05	1,303,788	17,444	245.67
ANT-12	0.5623	0.05	0.0025	3,426,868	45,850	1130.1
ANT-13	0.5623	0.05	0.025	169,467	2267	565.6
ANT-14	0.5623	0.05	0.0375	86,341	1155	498.9
ANT-15	0.5623	0.05	0.0625	50,768	679	476.68
ANT-16	0.5623	0.05	0.075	21,205	284	566.78
ANT-17	0.5623	0.05	0.0875	16,369	219	536.67
ANT-18	0.5623	0.05	0.1	7779	104	386.8
ANT-19	0.5623	0.0125	0.0025	658	9	209.5
ANT-20	0.5623	0.025	0.0025	58,296	780	702.8
ANT-21	0.5623	0.0375	0.0025	122,527	1639	735.1
ANT-22	0.5623	0.0625	0.0025	174,474	2334	814.56
ANT-23	0.5623	0.075	0.0025	260,214	3482	768.5
ANT-24	0.5623	0.0875	0.0025	203,459	2722	732.4
ANT-25	0.5623	0.1	0.0025	103,510	1385	345.7
ANT-26	0	0.05	0.0025	3551	48	326.5
ANT-27	0.3548	0.05	0.0025	4865	65	335.5
ANT-28	1.778	0.05	0.0025	5617	75	343.56
ANT-29	17.78	0.05	0.0025	8765	117	607.56
ANT-30	177.982	0.05	0.0025	702,20	940	643.89
ANT-31	562.34	0.05	0.0025	100,319	1342	632.3
ANT-32	0.5623	0.05	0.0015	4,626,769	94,342	1094.5

[a]S/A ratio: Potassium acrylate/Acrylic acid (ANT-1 to ANT-25 and ANT-32) and ammonium acrylate/acrylic acid (ANT-26 to ANT-31) Constant amounts of acrylic acid (1.27M) and KPS (0.009M) were taken in all the experiments for a polymerization volume of 40 mL. Where $\overline{M_c}$ = average molecular weight between crosslinks q = crosslink density.

potassium acrylate (KA), ammonium acrylate (AMA), *N*-isopropyl acrylamide(NIPAAm), and a tri functional crosslinker trimethylolpropane triacrylate (TMPTA) through free radical copolymerization and its subsequent evaluation for its absorption-release characteristic of water and fertilizer for agricultural use to conserve water by minimizing irrigation frequency and protect soil from the overdose of fertilizers. The synthesized polymers were designated as ANT-1 to ANT-32(Table I).

EXPERIMENTAL

Materials
Acrylic acid (AA, Himedia, Mumbai) and potassium persulphate (KPS, NICE, Cochin) used after purification by vacuum distillation (700 mmHg) and recrystallization with double distilled water,

respectively. Trifunctional crosslinker, trimethylolpropane triacrylate (TMPTA, Himedia Mumbai), *N*-isopropyl acrylamide (NIPAAm, Aldrich), *n*-heptane (NICE, Cochin), acetone, methanol, potassium hydroxide, ammonium hydroxide (Rankem, New Delhi), Water Keep, and Water Lock G 500 (Grain processing corporation, USA), urea, diammonium phosphate (DAP) and potash (SPIC) were purchased and used as received. Potassium acrylate (KA) and ammonium acrylate (AMA) were prepared by neutralization of acrylic acids with the corresponding bases. Sand, red, and clay soils were collected from the local fields.

SAP Synthesis
Polymer hydrogels from various proportions of monomers (Table I) were prepared by free radical copolymerization of AA, KA/or AMA, NIPAAm, and TMPTA using KPS initiator, at 70°C

in aqueous solution (40 mL) in a 50 mL stoppered borosilicate tube after deaeration by oxygen free nitrogen purging. The required amount of KA/or AMA was prepared by partially neutralizing the AA, using a known equivalent of KOH/or NH4OH under ice cold condition. The percent conversion monitored gravimetrically was >95% for a polymerization time around 10 min. The very high rate of polymerization was due to Trommsdorff–Norrish effect[29] (gel effect) and N-isopropyl acrylamide catalyzed radicalic decomposition of persulphate.[30,31] After the polymerization the polymer hydrogel obtained was recovered by repeatedly washing with ice cold methanol immediately to check the reaction and to remove unreacted monomers. The cross-linked gels thus obtained were cut into small pieces and dried to constant weight at 50°C under vacuum. The dry polymer gel was powdered and further purified by Soxhlet extraction using acetone–methanol (1 : 1 v/v), at 50°C for 3–4 days, powdered, sieved (mesh size 100 and 150 micron) and stored after vacuum drying.

Characterization of SAP

Fourier Transform-Infrared (FTIR) Spectroscopy. FTIR spectra of SAPs were recorded on KBr pellet for the spectral range 400–4000 cm^{-1} using Shimadzu FTIR-8400S by accumulating 48 scans at a resolution of 2 cm^{-1}.

Thermogravimetry (TG/DTG). TG/DTG studies were performed on TGA Q 500 V20.10 Build 36 with a sample size of 1.5–3.5 mg under air at a heating rate of 10°C/min for the temperatures ranging from ambient to 800°C.

Total Dissolved Solids (TDS). Total water soluble solids in soils were measured in terms of TDS values of the water extracts of the soils (10 g each) using a known volume (100 ml) of double distilled water, using DiST 1 Hanna TDS meter with automatic temperature compensation at 27°C.

Swelling Measurements

The degree of swelling of synthesized SAPs were measured both in distilled water and in fertilizer solutions (urea, diammonium phosphate, and potash) using the tea bag method.[32] A tea bag (i.e., a 100 mesh nylon screen) with average mesh size in the range (100–150 micron) containing an accurately weighed powdered and sieved sample (0.1 g) was immersed in 200 mL aqueous fertilizer solutions (0, 1, 2, 3, 4, and 5 wt %) taken in a thermostated vessel (27°C) and allowed to equilibrate (4 h). Then the tea bag was taken out from the solution and the excessive water adhering to the gel surface was removed superficially with tissue paper. The swelling profiles were constructed by plotting the water-absorbed during various time intervals at 27°C against time for typical samples (ANT-1 to ANT-24 & ANT-32), and at different temperatures for ANT-12. The initial slope of this plot (upto 60% swelling) was taken as the rate (R-mol/min) of absorption. The absorbency was calculated as amount (g) of water absorbed per gram of SAP. The equilibrium swelling (ES) was calculated by taking an average of three absorption measurements using the eq. (1)

$$ES = (W_s - W_d)/W_d \qquad (1)$$

where W_s and W_d are the weights of the swollen gel and the dry sample, respectively. To obtain the water release and retention

behaviors, the above procedure was followed at 27°C and other temperatures. The AE values for swelling and deswelling were evaluated for the initial absorptions (up to 60%) and release of water at various temperatures assuming Arrhenius kinetics. For Arrhenius plot, log (R mol/min) for absorption and release was used instead of log k, where k is the rate constant for absorption or release. The swellability of ANT-12 under irrigated sand, red and clay soils were also evaluated for field applications. This was done by taking 1 kg each of the respective soil in separate plastic trays (28 × 22 × 6 cm^3) and uniformly distributed inside the tray followed by sowing 1 g of powdered and sieved SAP sample uniformly on each soil surface. Then additional 1 kg of each soil was uniformly spread over the SAP amended respective soil taken in the plastic tray followed by the uniform pouring of one liter (V_a) distilled water to each soil under ambient conditions and allowed to equilibrate(4 h). The unabsorbed water (V_u) stagnating at the soil surface was syringed out carefully and quantified. Then the water absorbed ($V_a - V_u$) by each soil was calculated. Control (blank) experiment was also conducted similarly without polymer for each soil and the volume (V_c) of absorbed water in control was determined. From these data, water absorbed by the polymer [($V_a - V_u$) − V_c] under soil was calculated and given in Table IV. The soil experiment was also repeated using commercial SAP samples namely Water Keep and Water Lock (USA) and the data were included in Table IV.

Molecular Weight Between Crosslinks ($\overline{M_c}$)

Crosslinked SAP was allowed to attain ES in double distilled water as described earlier and its weight (W) was determined. The polymer volume fraction υ_1 of the swollen polymer was calculated[33] using eq. (2)

$$\upsilon_1 = \frac{W_0 \rho_w}{W\rho - W_0(\rho - \rho_W)} \qquad (2)$$

where W_0 is the initial weight of the sample and W is weight of swollen polymer, ρ and ρ_w are the density of dry crosslinked SAP and water at 27°C, respectively. The density of the polymer was determined in a pycnometer[34] using n-heptane. The polymer volume fraction υ_1 was used to estimate the average molecular weight between cross links ($\overline{M_c}$)[33] employing the Flory–Rehner eq. (3)

$$\overline{M_c} = \rho V_1 \frac{\upsilon^{1/3} - 2\upsilon_1/f}{\ln(1 - \upsilon_1) + \upsilon_1 + \chi\upsilon_1^2} \qquad (3)$$

where V_1 is the molar volume of water (18.062 cm^3/mol), χ is the polymer-solvent interaction parameter, and "f" is the crosslinking functionality. In swollen SAPs, the thermodynamics of interaction was measured in terms of polymer–solvent interaction parameter χ, which indicates the change of interaction energy when polymer and solvent are mixed together. In polymer–water systems, the higher the value of χ the weaker is the interaction between polymer and water, and stronger is the interaction between hydrophobic groups or between polymer chains.

The value of χ was calculated[35] using the eq. (4)

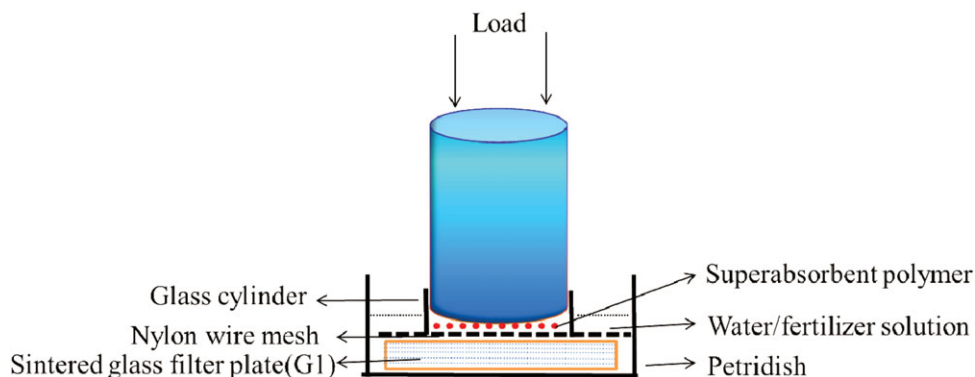$$\chi \cong \frac{1}{2} + \frac{\upsilon_1}{3} \qquad (4)$$

Figure 1. Experimental set up for measuring water absorbency of SAP under load. [Color figure can be viewed in the online issue, which is available at wileyonlinelibrary.com.]

Determination of Crosslinking Density (q)

Crosslink density is an important parameter that will significantly influence the swelling and deswelling characteristics of SAP. Hence this was calculated[34] using the eq. (5)

$$q = \frac{\overline{M_c}}{M_r} \qquad (5)$$

where M_r the molar mass of the repeat unit was determined[34] using the eq. (6)

$$M_r = \frac{m_{AA}M_{AA} + m_{KA}M_{KA} + m_{NIPAAm}M_{NIPAAm}}{m_{AA} + m_{KA} + m_{NIPAAm}} \qquad (6)$$

where m_{AA}, m_{KA}, and m_{NIPAAm} are the masses and M_{AA}, M_{KA}, and M_{NIPAAm} are the molar masses of the respective monomers.

Absorbency Under Load (AUL)

Under field applications, SAP may encounter significant stress from the weight of the soil that may affect the swellability of SAP. Hence, the water-uptake of SAP was also evaluated under load. This was done by mounting a nylon mesh having a known weight of dry SAP ANT-12 (0.1 g) on a porous sintered glass filter plate (dia 80 mm and thickness 7 mm) placed in a petri dish ($d = 118$ mm, $h = 12$ mm). The SAP was pressurized by applying a known load (1, 2, 3, 4, and 5 tons) via a stainless steel cylinder ($d = 74$ mm, $h = 50$ mm) kept on the SAP for 60 min (Figure 1). The measurement was done in an enclosure to minimize water loss. After this, the swollen particles were weighed and AUL was calculated[36] using eq. (1).

Fertilizer Release

To investigate the release of the fertilizer, 0.5 g of fertilizer loaded powdered SAP was placed in 100 mL of double distilled water at 27°C to facilitate the fertilizer release. After every two days, 2 mL from this solution was pipetted out and its fertilizer content was determined gravimetrically by vacuum drying at 60°C. From this the percentage of the fertilizer released was calculated[37] using the eq. (7)

% of fertilizer released

$$= \frac{(\Delta W)n \times [100 - (n-1) \times 2]/2 + \sum_{i=1}^{n-1}(\Delta W)_i}{W_o} \qquad (7)$$

where $(\Delta W)_i$ is the weight of fertilizer released from the ith 2 mL sample, W_0 is the amount of fertilizer loaded in SAP and n indicates the number of fertilizer release measurements at various time intervals in a single experiment.

RESULT AND DISCUSSION

Mechanism of Polymerization

Synthesis of SAP by free radical mechanism involved initiation, propagation, and termination steps as indicated in Scheme 1. Crosslinking occurred between two growing polymer chain radicals through the tri functional crosslinker (Scheme 1). The termination may occur either by coupling/disproportionation of growing polymer radicals or by chain transfer through monomer/ or polymer or solvent and by primary radical.[38] Termination through the disproportionation of growing polymer radicals will introduce terminal double bond in the dead polymer.

Characterization of SAP

FT-IR Analysis. Representative FT-IR spectra of SAPs (ANT-12, ANT-18, and ANT-26) are displayed in Figure 2. The assignments of the prominent absorption peaks observed from the FTIR spectra of SAPs are shown in Table II. Analysis of this data[39] indicated the presence of monomer and crosslinker moieties in the synthesized SAP. For an example the absorption peaks at 1730 and 1550 cm^{-1} in all the SAPs were attributed to the presence of >C=O stretching of ester group (TMPTA), and carboxylate anion (KA), respectively.

Thermogravimetric (TG) Analysis. TG thermograms for representative SAP samples (ANT-1, ANT-11, ANT-12, and ANT-15) displayed in Figures 3 and 4 showed multistep degradations. The initial weight loss up to 150°C was attributed to the residual moisture content in the polymer. The multistep degradation above 210°C are more likely due to the degradation initiated via the olefinic bonds,[40] saturated terminal ends, decarboxylation of carboxylate anion and scission of crosslinks etc. SAP prepared with KA as a comonomer showed an enhanced degradation temperature (ANT-11) as compared to the one prepared without KA (ANT-1, Figure 3). This was also supported by the higher AE for SAP containing KA (Table III). The major degradation of SAP (ANT-11) around 350°C was more likely attributed to the degradation initiated through decarboxylation of the carboxylate anion.[40]
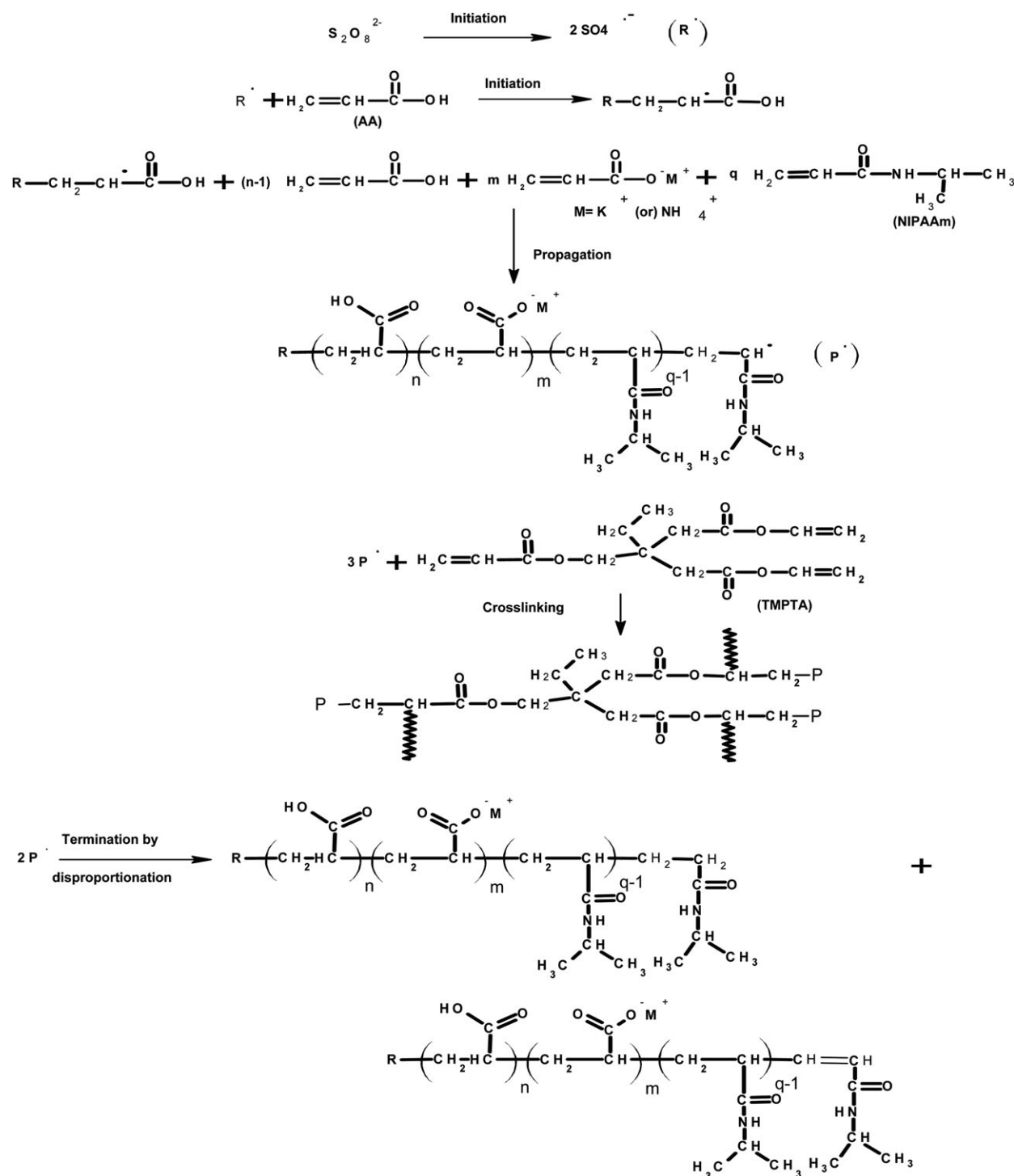
Scheme 1. The mechanism of radical copolymerization in SAP synthesis.

Even though the TG traces of both ANT-12 and ANT-15 showed five step degradations (Figure 4), the corresponding temperatures and the percentage weight loses for these degradation steps were different because of the variation in their crosslink density values. For example the second step degradation temperature (380°C) for ANT-15 was greater than that (370°C) of ANT-12 roughly by 10°C. But the temperatures for the first step degradation were nearly the same for both SAPs. This implied that ANT-15 showed more resistance towards thermal degradation in the second step, which may be attributed to the higher crosslink density of ANT-15 than that of ANT-12. This was also supported by the higher mass residue (30%) at 900°C for ANT-15 as compared to that (15%) of ANT-12.
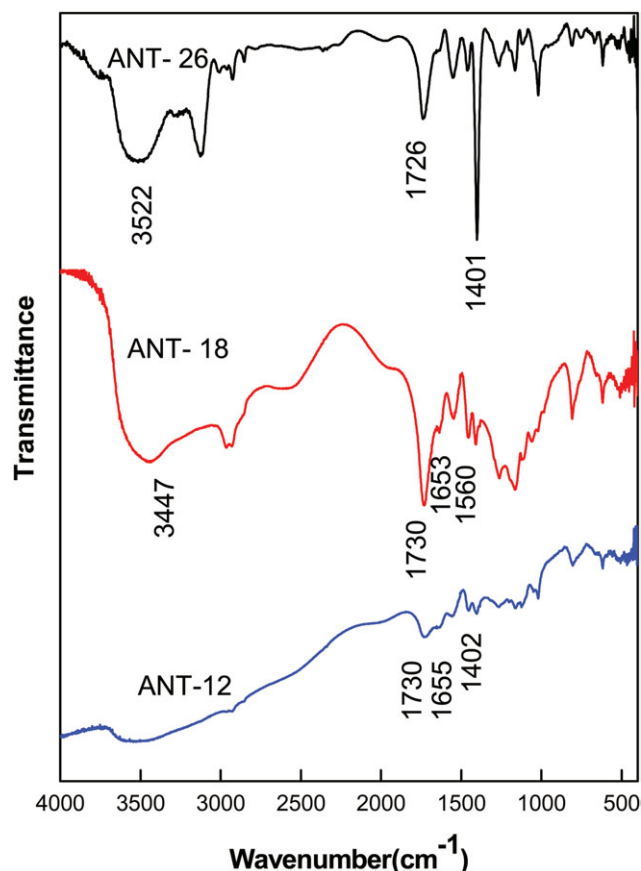
Figure 2. FTIR spectra of ANT-12, ANT-18, and ANT-26. [Color figure can be viewed in the online issue, which is available at wileyonline library.com.]
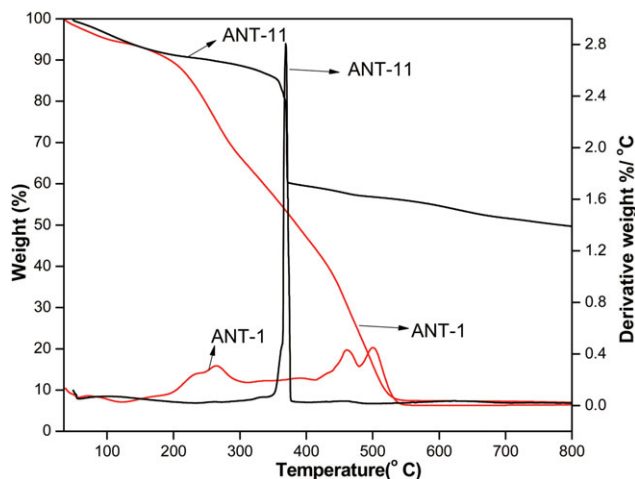

Figure 3. TG/DTG traces of ANT-1 and ANT-11. [Color figure can be viewed in the online issue, which is available at wileyonlinelibrary.com.]

Thermo Kinetic Data

The kinetic data such as order and AE (Table III) for thermal degradation of SAPs were determined using the weight loss data from the TG trace through the Freeman and Carroll eq. (8)

$$\log_{10}\left\{\frac{1-(1-\alpha)^{1-n}}{T^2(1-n)}\right\} = \log_{10}\frac{AR}{\alpha E}\left[1-\frac{2RT}{E}\right] - \frac{E}{2.3RT} \quad (8)$$

for all values of n except $n = 1$

a plot of $\log_{10}\left\{\frac{1-(1-\alpha)^{1-n}}{T^2(1-n)}\right\}$ against $\frac{1}{T}$, a plot of $-\log_{10}\left\{\frac{-\log_{10}-(1-\alpha)^1}{T^2}\right\}$ against $\frac{1}{T}$ for $n = 1$ and

a plot of $Y = -\log_{10}\left\{\frac{1-(1-\alpha)^{1-n}}{T^2(1-n)}\right\}$ against $\frac{1}{T}$ for $n = 0, \frac{1}{2}$ and $\frac{2}{3}$

Table II. FTIR Spectral Data for Synthesized Typical SAP Samples

| Bonds and their frequency range (cm^{-1})	Observed typical frequencies of SAP										
	ANT-1	ANT-6	ANT-11	ANT-12	ANT-15	ANT-18	ANT-19	ANT-22	ANT-26	ANT-29	ANT-31
Amide >NH stretching (3500–3400)	3446	3446	–	3456	3450	3447	3450	3439	3522	3463	–
C=O stretching (Amide I) (1650)	1652	1683	1645	1655	1647	1653	1654	1649	1636	1638	1648
Aliphatic —CH$_2$ stretching (2926–2853)	2928	2950	2927	2928	2932	2962	2949	2962	2932	2920	–
>C=O stretching in —C(=O)O— (1610–1550)	1548	1563	1559	–	1543	1560	1563	1583	1533	1542	1568
Ester >C=O stretching (1750–1735)	1732	1719	–	1730	1729	1730	1708	1718	1726	1721	1728
>C—O stretching (1300–1100)	1164	1164	1171	1163	1169	1165	–	1152	1170	–	–
Hydroxyl free —OH stretching (3650–3590)	3558	3584	–	3560	3565	3589	3526	3610	3640	3578	3130
—COOH >C=O bending (1420)	1455	1450	–	1402	1454	1453	1457	1404	1401	1400	1401
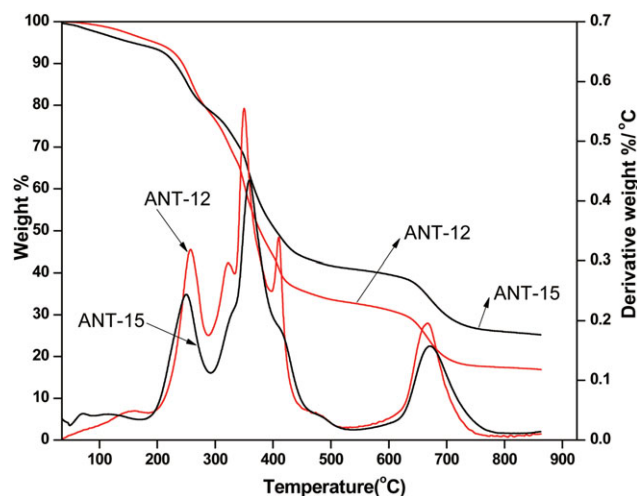
Figure 4. TG/DTG traces of ANT-12 and ANT-15. [Color figure can be viewed in the online issue, which is available at wileyonlinelibrary.com.]
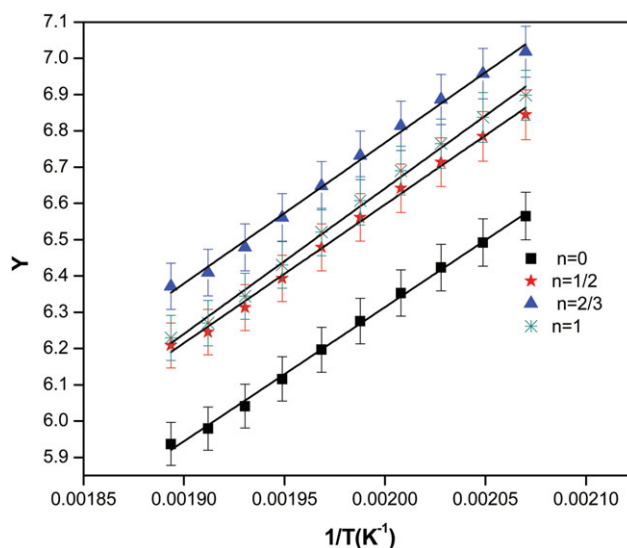

Figure 5. Modified Arrhenius plots for thermal degradation of ANT-12 from TG data. [Color figure can be viewed in the online issue, which is available at wileyonlinelibrary.com.]

should result in a straight line of slope $- (E/2.3 \; R)$ for the correct value of n. The kinetic order (n) and AE were determined from best fit of Y vs. $1/T$ (Figure 5) for different values of n and from the corresponding slope values, respectively for the polymer ANT-12. These data were also calculated for ANT-1, ANT-11, and ANT-15 and given in Table III. The order for the best fit appeared to be zero for all these samples and the corresponding AEs were found to be 22.6, 470.5, 70.8, and 57.3 kJ/mol (Table III), respectively. Analysis of data in Table III indicated that the first step thermal degradation of SAP followed zero order kinetics.[41]

Table III. Kinetic Parameters for Thermal Degradation of ANT-1, ANT-11, ANT-12, and ANT-15

SAP code	'n' values	Activation energy[a] (kJ/mol)	Order
ANT-1	0	22.574	Zero
	1/2	36.418	
	2/3	40.152	
	1	39.405	
ANT-11	0	470.522	Zero
	1/2	443.889	
	2/3	416.757	
	1	427.728	
ANT-12	0	70.768	Zero
	1/2	73.065	
	2/3	74.271	
	1	76.761	
ANT-15	0	57.269	Zero
	1/2	60.103	
	2/3	60.754	
	1	62.113	

[a]Activation energies were calculated in the lower degradation temperature range (up to 250°C).

Water and Fertilizer Uptake and Release Studies

Water and fertilizer (urea) uptake, and release profiles with respect to time for the optimized SAP sample ANT-12 are given in Figure 6. The profiles revealed that the water and fertilizer solution uptake rates were greater than the corresponding release rates. The decrease in the release rate was more in presence of fertilizers than in pure water. This may be due to the enhanced physical crosslinking through H-bonding network involving urea, water and SAP. The SAP ANT-12 had absorbed 1.130 kg of pure water per gram at 27°C. The percentage uptake of fertilizers viz., urea, DAP and potash per gram of ANT-12 were 75, 57, and 42, respectively from their 1% solutions. The study demonstrated that the equilibrium swelled SAP had
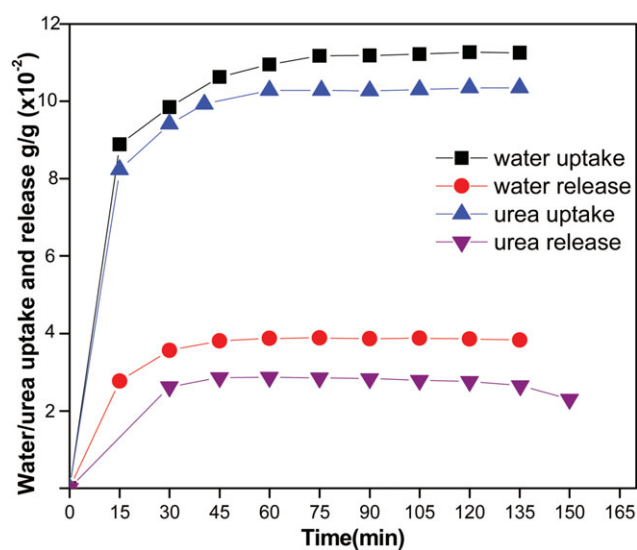

Figure 6. Water and fertilizer (urea) uptake, and release profiles for ANT-12. [Color figure can be viewed in the online issue, which is available at wileyonlinelibrary.com.]
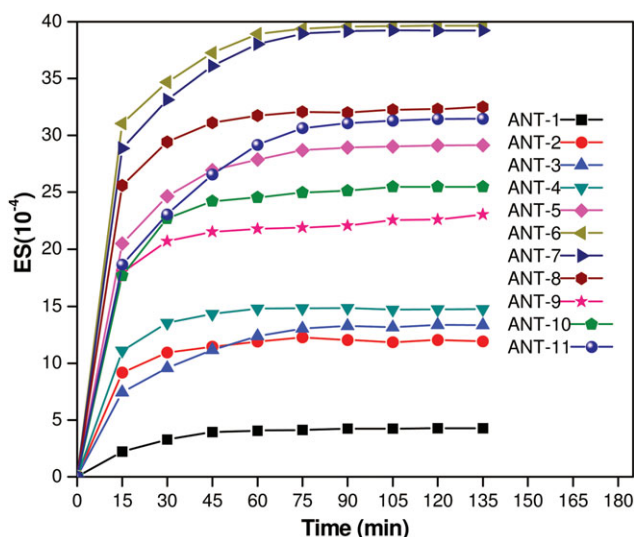
Figure 7. Time variation of swellability for various mole ratios of KA and AA. [Color figure can be viewed in the online issue, which is available at wileyonlinelibrary.com.]

released the absorbed water completely over a period of 30 days, whereas only 52, 38, and 30% of urea, DAP and potash, respectively were released over a period of 22 days under ambient laboratory conditions from the fertilizer loaded ANT-12 in single cycle in a controlled fashion. The mechanism of water and fertilizer solution release from swelled ANT-12 was analyzed using the power law[42] eq. (9)

$$\frac{Mt}{M\infty} = kt^n \qquad (9)$$

where, M_t = amount of the water/fertilizer released by polymer at time t, M_∞ = amount of the water/fertilizer released after infinite time, k = constant and n = diffusion exponent

The values of diffusion exponents (n) were found to be in the range 0.2–0.3 and 0.34–0.41 for water and fertilizer solutions, respectively. These values implied that the release mechanism appeared to be nonFickian.[42]

Factors Affecting Swellability
Monomer Feed Composition
Acrylic acid salt and acrylic acid ratio (S/A), NIPAAm, and crosslinker. The nature and percentage of monomers incorporated in SAP will influence its water absorption characteristics. The profiles for water absorption in terms of water uptake (g/g) vs. time for typical SAPs (ANT-1 to ANT-11) with various values of S/A are given in Figure 7. The plots indicated that increasing the concentration of KA in the feed had enhanced the water absorption capacity of the formed hydrogel, and this attained a maximum value when S/A = 0.0509. For S/A values >0.05, a reduction in water up-take was noticed. This was mainly attributed to the more hydrogen bonding at lower values of S/A and osmatic pressure effect.[43] In addition, at S/A values >0.0509, physical crosslinking via H-bonding may be reduced. The water absorption profiles with respect to time for typical SAPs prepared using different concentrations of NIPAAm are displayed in Figure 8. Increased concentration of NIPAAm in the feed displayed an increased water uptake for low S/A values in the feed. The swellability of the synthesized SAPs prepared using low concentration of NIPAAm showed a decrease in ES because of the weakening of the hydrogen bonding between the carboxylic groups and water, and synergistic effect of the different hydrophilic groups.[44] ES increased upto an optimum concentration of NIPAAm (0.05M) and decreased with increase of NIPAAm beyond (0.05M).

Crosslinking density, a key factor affecting the water absorbency of superabsorbents was directly proportional to crosslinker concentration for its low values and inversely proportional to it at higher concentrations.[45] Since the water absorbency can be
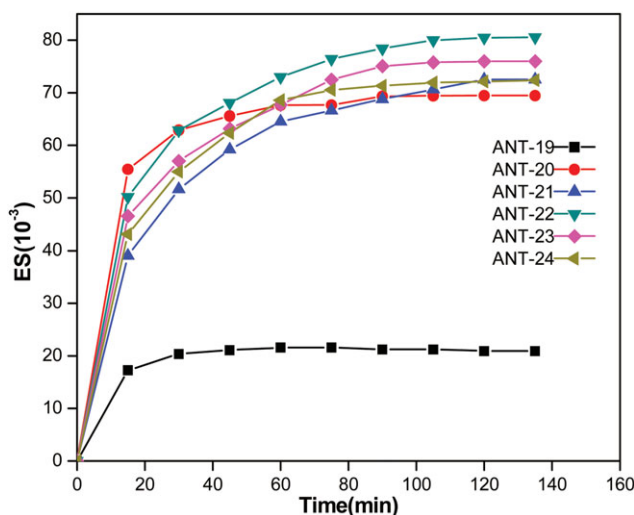

Figure 8. Effect of [NIPAAm] in feed on swellability of SAP. [Color figure can be viewed in the online issue, which is available at wileyonline library.com.]
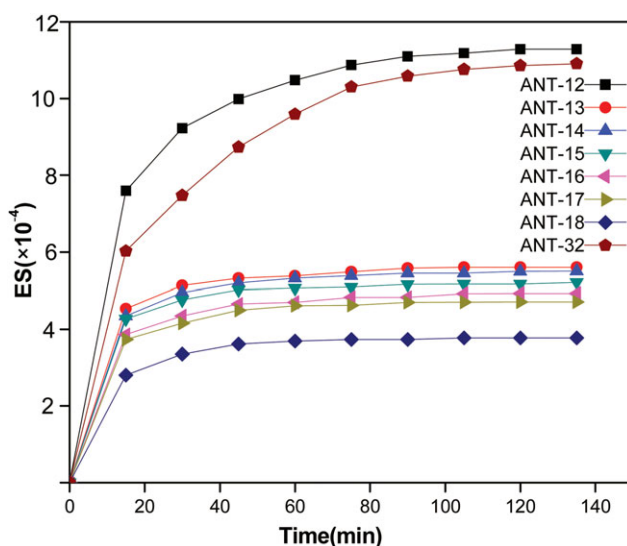

Figure 9. Effect of [TMPTA] in feed on swellability of SAP. [Color figure can be viewed in the online issue, which is available at wileyonline library.com.]
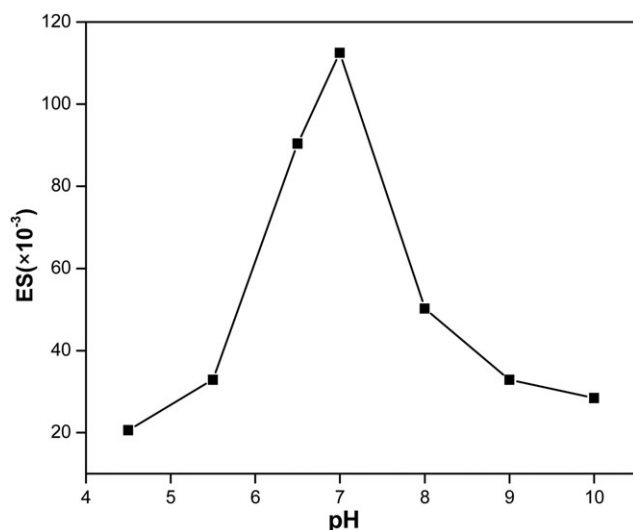
Figure 10. Effect of pH on swellability of ANT-12.

altered with a small change in crosslinker concentration in feed, hydrogel network with different crosslinker levels were prepared and evaluated by their water absorption and release characteristics. The influence of crosslinker level on water uptake profiles of typical SAP are shown in Figure 9. When the crosslinker concentration was 0.0025M, water absorbency had increased to the maximum value 1130 g/g. For crosslinker concentration >0.0025M in the feed water absorbency decreased drastically. This could be attributed to the poor physical crosslinking at higher crosslinker level.

With the increased crosslinker concentration beyond 0.0025M (Table I, ANT-12 to ANT19) for the constant concentrations of other ingredients both the water uptake and crosslink density decreased. At crosslinker level >0.0025M the formed hydrogel network may have decreased space among the grids of the three-dimensional network.[46] This would make it more difficult for the network to be swollen by water, which was responsible for the decrease in water absorbency.[46] This also revealed that physical crosslinking might have significantly influenced both the water uptake and crosslink density. For the various concentrations of the crosslinker below 0.0025M at constant concentrations of other ingredients, a decrease both in water uptake and crosslink density was observed. Only a typical sample data (ANT-32) was furnished in the Table I for these concentrations of the crosslinker. A similar explanation can be offered for the variation in water uptake, crosslink density and average molecular weight between crosslinks for varying concentration of N-isopropyl acrylamide for constant concentrations of other ingredients.

Physical Parameters

pH. Ionic superabsorbent hydrogels exhibit different swelling behavior at different pH levels and the swelling profile for ANT-12 is given in Figure 10. In the present investigation the ES for the hydrogel ANT-12 was studied in buffers of different pH values. Maximum swelling (1130 g/g) was observed at pH 6.9. For pH values nearer to neutral and slightly basic conditions most of the carboxylate groups are ionized and the electrostatic repulsion between —COO⁻ groups may cause an

enhancement of the swelling capacity of SAPs.[35] At different acidic pH values (pH 4.5, 5.5, and 6.0), most of the carboxylate groups are protonated, so the main anion–anion repulsive forces may be eliminated, which may result in the collapse of hydrogel. This might have resulted in the reduction of swelling values to 208, 335, 904 g/g, respectively. At pH value >9.0 the swelling was drastically reduced to 124 g/g due to repulsive forces among carboxylate anion.[47,48]

Particle size. The ultimate swelling capacities and ES rate of hydrogels will be increased with decreasing particle size, most likely as a result of the increase in specific surface area accessible to the water.[49] In this present investigation a SAP with 150–100 μ sizes had absorbed 1130 and 1023 g of water per gram of ANT-12, respectively.

Temperature. The effect of the temperature on the water absorbency of the super absorbents was investigated for the temperatures range 20–55°C. The temperature profiles for water absorption of ANT-12 are given in Figure 11. With the increased temperature for the temperature range 20–30°C the initial swelling rate had increased. A maximum absorbency of 1025 g/g was observed at 30°C and its value at 20°C was 985 g/g. The observed increased rate and extent of swelling in the temperature range 20–30°C were attributed to the factors such as flexibility of polymer chains and diffusion of water molecules into SAP backbones that might have improved with increased temperature.[35] The decreased water absorption for temperatures beyond 30°C could be attributed to the temperature dependence association/dissociation of the hydrogen bonding by the hydrophilic groups in the copolymer.[50] The Arrhenius plots for water absorption and release for the temperature range 20–55°C are shown in Figure 12. The plots tend to imply that the absorption and release of water found to possess two AEs corresponding to the different temperature regions 20–30°C and 35–55°C. The AEs calculated from slope of the Arrhenius plots obtained from the linear fit of the data for water uptake and release for ANT-12 under these temperature regions were found to be 4.8 and
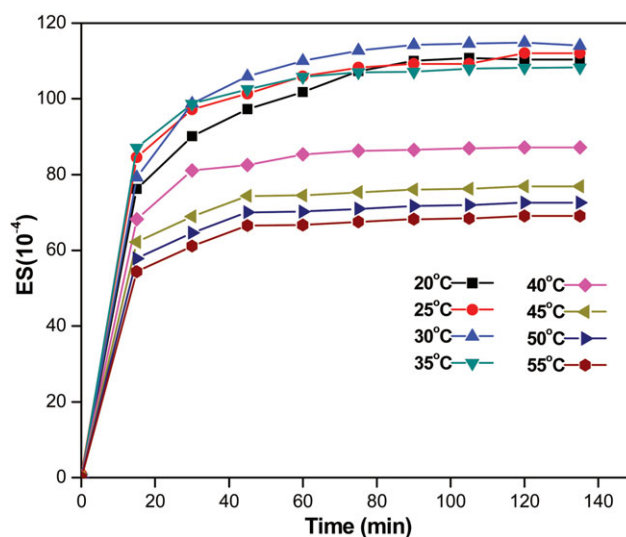

Figure 11. Temperature effect on swellability of ANT-12. [Color figure can be viewed in the online issue, which is available at wileyonlinelibrary.com.]
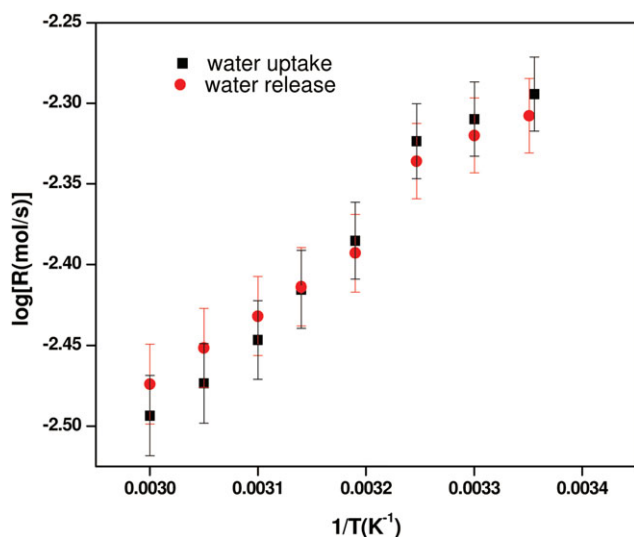
Figure 12. Arrhenius plots for water absorption and release by ANT-12. [Color figure can be viewed in the online issue, which is available at wileyonlinelibrary.com.]

5.2 kJ/mol, and 11.1 and 8.1 kJ/mol, respectively. AE values indicated that the rate of water absorption was slower than the rate of release at elevated temperatures (35–55°C) and rate of water release was slower than the rate of absorption for ambient temperatures (20–30°C).

Ionic strength. The water absorbency of the hydrogel in aqueous fertilizer solutions such as urea, potash, and diammonium phosphate for various concentrations (0, 1, 2, 3, 4, and 5%) taken in a thermostated vessel at 27°C decreased with increased ionic strength of the fertilizer solutions. The time profiles for water and fertilizer uptake for various concentrations of urea fertilizer for ANT-12 are given in Figure 13. The profiles revealed that with the increased concentrations of fertilizer, the SAP swellability decreased. This is in accordance with the
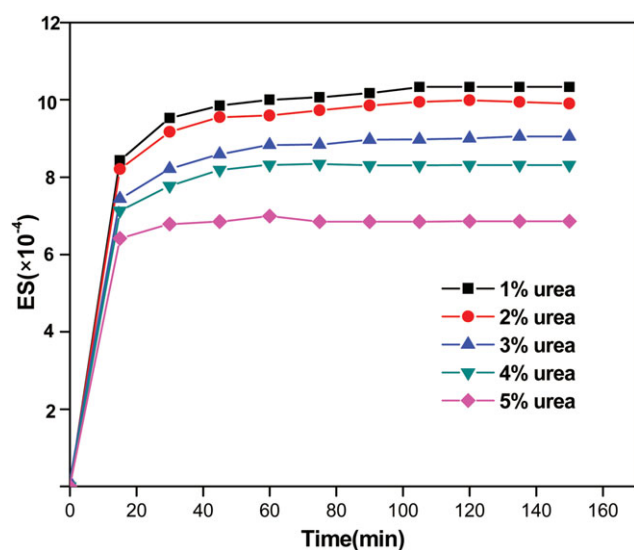
reported[35] results that the swelling values for all "anionic" hydrogels may decrease in saline and fertilizer media. This undesired swelling loss has been attributed to the "charge screening effect" of the cations leading to the reduction of osmotic pressure, the driving force for swelling between the gel and the aqueous phases of the solution.[35]

Analysis of TDS Data

The comparison of the TDS values of the extracted water from the water saturated sand, red, and clay soils with the absorption values of these water extracts and pure water by ANT-12 (Table IV) indicated that the increased TDS values decreased the water uptake. For an example the reduction of water uptake in the water extracts of sand, red, and clay soils were 20, 33, and 40%, respectively. The reduction in water uptakes under irrigated respective soils were 64, 77, and 80%. The greater loss in water uptake under the above soils as compared to those in pure water and water extracts of these soils could be attributed to the introduction of additional crosslinks in SAP via the water soluble Ca^{2+}, Mg^{2+}, and Al^{3+} salts present in the irrigated soil.[51]

Influence of Stress on Swellability of SAP

The swellability of ANT-12 varied with respect to the applied pressure on SAP particle and it is shown in Figure 14, which revealed that if the applied load is enhanced to 5 t on SAP, the water uptake becomes zero. This observation indicated that the synthesized SAP was capable of picking-up water below an applied load of 5 t only.

Swellability of SAP Under Soil

The water absorbed by 1 g ANT-12 under sand, red, and clay soils shown in Table IV implied that they decreased to 399, 256, and 223 mL of water per gram of polymer under laboratory conditions as compared to those values in pure water. But these values were very much higher than those values observed for the commercial SAPs, Water Keep and Water Lock. The decreased water uptake under soil may be attributed to the decreased saturated hydraulic conductivity of the soils and increased ionic strength of water.[52] It was reported[53] that when

Figure 13. Dissolved fertilizer effect on swellability of ANT-12. [Color figure can be viewed in the online issue, which is available at wileyonlinelibrary.com.]
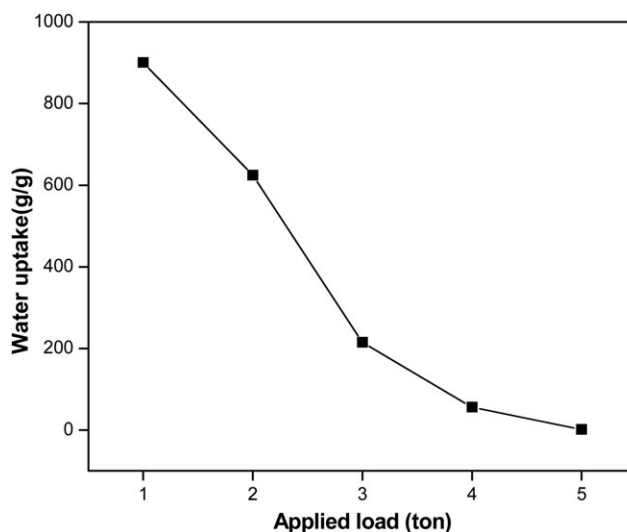

Figure 14. Swellability of ANT-12 under different load.

Table IV. Comparison of Swelling Behavior of ANT-12 with Commercial SAP

Nature of soil	pH	TDS[a] (ppm)	Water[b] uptake (g/g)	Water uptake under soil (g/g)		
				ANT-12	Water Keep	Water Lock
Sand	7.8	31	900	399	103	152
Red	8.1	53	761	256	58	87
Clay	8.3	78	688	223	25	54

[a]TDS of the water extract of sand, red soil, and clay soils. [b]Water uptake in extracted water from the soils.

SAP swells under soil, it reduced the largest pores in the soil especially in the sandy soils. The investigation demonstrated that application of SAPs into the soil increased its saturated water content, and water holding capacity.[54] Hence, the ANT-12 can be a potential candidate for agricultural applications.

Limitations of ANT-12 Under Field Applications

The swellability of ANT-12 was affected by TDS values, salinity of irrigated water[55,56] and the operation of soil pressure on it. At high applied load on ANT-12, the degree of swellability decreased in any medium and this could be attributed to shrinkage of polymer network.[57] Moreover, the efficacy of the SAP may decrease over a period of time and to compensate for these loses, higher degree of application rates may be required. These factors may affect the economic value of crops grown on fields amended with SAP. In addition SAPs are quite fragile and tend to break apart easily during repeated swelling and deswelling under soil, which may bring down their water retention capacity.[58]

CONCLUSIONS

SAPs of different compositions were synthesized free radically using AA, KA/AMA, and NIPAAm monomers with TMPTA crosslinker and evaluated for their water and fertilizer uptake and release, which followed a non-Fickian mechanism. The maximum water absorbed by 1 g of synthesized SAP(ANT-12) was 1.130 kg which was very much higher than those reported for commercial SAPs, such as Water Keep and Water Lock (USA). These values were decreased to 399, 256, and 223 g/g under sand, red, and clay soils, respectively. The water absorption was correlated with the crosslink density determined using Flory–Rehner equation. The synthesized SAP displayed controlled release of water and fertilizer over a period of 30 and 22 days, respectively after equilibrium absorption. TG results of SAP demonstrated a good thermal stability in air for using under soil. Analysis of the initial step thermal degradation of SAP(ANT-12) in TG revealed a zero order kinetics with an AE of 70.8 kJ/mol. The Arrhenius AE (8.1 kJ/mol) for release in the temperature range 35–55°C was less than that (11.1 kJ/mol) for absorption. But in the temperature range 20–30°C the AE (5.2 kJ/mol) for release was greater than that (4.8 kJ/mol) for uptake. The observed results demonstrated its candidature as a potential material to conserve water, fertilizer, and soil fertility in agricultural cultivations.

ACKNOWLEDGMENTS

REFERENCES

1. Kiatkamjornwong, S. *Sci. Asia.* **2007**, *33*, 39.
2. Murali Mohan, Y.; Keshava Murthy, P. S.; Sreeramulu, J.; Mohana Raju, K. *J. Appl. Polym. Sci.* **2006**, *102*, 1.
3. Chen, J.; Park, H.; Park, K. *J. Biomed. Mater. Res.* **1999**, *44*, 53.
4. Dong, L. C.; Hoffman, A. S. *J. Control. Release* **1991**, *15*, 141.
5. Colombo, P. *Adv. Drug. Del. Rev.* **1993**, *11*, 37–57.
6. Kuzma, P.; Moo Young, A. J.; Moro, D. *Macromol. Symp.* **1996**, *109*, 15.
7. Mohana Raju, K.; Padmanabha Raju, M.; Murali Mohan, Y. *J. Appl. Polym. Sci.* **2002**, *85*, 1795.
8. Kohls, S. J.; Baker, D. D.; Kremer, D. A. *Plant. Soil.* **1999**, *214*, 105.
9. Raju, K. M.; Raju, M. P. *Polym. Int.* **2001**, *50*, 946.
10. Chen, P.; Zhang, W.; Luo, W.; Fang, Y. *J. Appl. Polym. Sci.* **2004**, *93*, 1748.
11. Sires, U. I.; Mallory, S. B. *Postgrad. Med.* **1995**, *98*, 79.
12. Gourmand, M.; Corpart, J. M. *J. M. Act. Chim.* **1999**, *11*, 46.
13. Jensen, O. M.; Hansen, P. F. *Cem. Concr. Res.* **2001**, *31*, 647.
14. Zendehdel, M.; Barati, A.; Alikhani, H. *Polym. Bull.* **2011**, *67*, 343.
15. Dadhaniya, P. V.; Patel, M. P.; Patel, R. G. *Polym. Bull.* **2007**, *58*, 359.
16. Atta, A. M.; Abdel-Rahman, A.; El Aassy, I.; Ahmed, F. Y.; Hamza, M. F. *J. Dispersion Sci. Technol.* **2011**, *32*, 84.
17. Atta, A. M.; El-Ghazawy, R. A. M.; Farag, R. K.; Abdel-Azim, A. A. *J. Polym. Res.* **2006**, *13*, 257.
18. Dzinomwa, G. P. T.; Wood, C. J.; Hill, D. J. T. *Polym. Adv. Technol.* **1997**, *8*, 767.
19. Gao, D.; Heimann, R. B.; Lerchner, J.; Seidel, J.; Wolf, G. *J. Mater. Sci.* **2001**, *36*, 4567.
20. Park, J. H.; Kim, D. *J. Appl. Polym. Sci.* **2001**, *80*, 115.
21. Karadag, E.; Uzum, O. B.; Saraydin, D. *Eur. Polym. J.* **2002**, *38*, 2133.
22. Dorraji, S. S.; Golchin, A.; Ahmadi, S. *Clean Soil Air Water* **2010**, *38*, 584.
23. Geesing, D.; Schmidhalter, U. *Soil Use Manage.* **2004**, *20*, 207.
24. Ingram, D. L.; Yeager, T. H. *J. Environ. Hort.* **1987**, *5*, 19.

25. Huttermann, A.; Orikiriza, L. J. B.; Agaba, H. *Clean Soil Air Water* **2009**, *37*, 517.

26. Sing, B.; Sekhon, G. S. *Agr. Environ.* **1979**, *4*, 207.

27. Almasri, M. N.; Kaluarachchi, J. J. *J. Environ. Manage.* **2005**, *74*, 365.

28. Van den Brandt, H. M. P.; Smit, H. P. *Environ. Pollut.* **1998**, *102*, 705.

29. Achilias, D. S.; Kiparissides, C. *Macromolecules.* **1992**, *25*, 3739.

30. Subramanian, K. *Eur. Polym. J.* **2001**, *37*, 55.

31. Hunkeler, D. *Macromolecules.* **1991**, *24*, 2160.

32. Pourjavadi, A.; Bardajee, G. R.; Soleyman, R. *J. Appl. Polym. Sci.* **2009**, *112*, 2625.

33. Bertoldo, M.; Bronco, S.; Gragnoli, T.; Ciardelli, F. *Macromol. Biosci.* **2007**, *7*, 328.

34. Yarimkaya, S.; Basan, H. *J. Macromol. Sci. Pure Appl. Chem.* **2007**, *4*, 939.

35. Pourjavadi, A.; Barzegar, S. *Starch* **2009**, *61*, 161.

36. Marandi, G. B.; Esfandiari, K.; Biranvand, F.; Babapour, M.; Sadeh, S.; Mahdavinia, G. R. *J. Appl. Polym. Sci.* **2008**, *109*, 1083.

37. Teodorescu, M.; Lungu, A.; Stanescu, P. O.; Neamtu, C. *Ind. Eng. Chem. Res.* **2009**, *48*, 6527.

38. Subramanian, K.; Shanmuganandha Moorthy, K.; Kishore, K. *Polymer*, **1997**, *38*, 527.

39. El-zahhar, A. A.; Abdel-Aziz, H. M.; Siyam T. *J. Macromol. Sci. Pure Appl. Chem.* **2007**, *44*, 215.

40. Yu, C.; Hui-min, T. *Carbohydr. Res.* **2006**, *341*, 887.

41. Coats, A. W.; Redfern, J. P. *Nature* **1964**, *201*, 68.

42. Hosseinzadeh, H. *J. Chem. Sci.* **2010**, *122*, 651.

43. Mahdavinia, G. R.; Pourjavadi, A.; Hosseinzadeh, H.; Zohuriaan, M. J. *Eur. Polym. J.* **2004**, *40*, 1399.

44. Suo, A.; Qian, J.; Yao, Y.; Zhang, W. *J. Appl. Polym. Sci.* **2007**, *103*, 1382.

45. Flory, D. J. Principles of Polymer Chemistry; Cornell University Press: Ithaca, New York, **1953**.

46. Wu, L.; Liu, M. *Polym. Adv. Technol.* **2008**, *19*, 785.

47. Mahkam, M.; Sharifi-Sanjani, N. *Polym. Degrad. Stab.* **2003**, *80*, 199.

48. Mahkam, M.; Mohammadi, R.; Assadi, M. G.; Ranaei-Siadat, S. O.; Barshan, M.; Ranaei-Siadat, S. E. *Silicon Chem.* **2006**, *3*, 51.

49. Omidian, H.; Hashemi, S. A.; Sammes, P. G.; Meldrum, I. G. *Polymer* **1999**;*40*, 1753.

50. Murali Mohan, Y.; Keshava Murthy, P. S.; Mohana Raju, K. *React. Funct. Polym.* **2005**, *63*, 11.

51. Chatzoudis, G. K.; Rigas, F. *Commun. Soil. Sci. Plant Anal.* **1999**, *30*, 2465.

52. Andry, H.; Yamamoto, T.; Irie, T.; Moritani, S.; Inoue, M.; Fujiyama, H. *J. Hydrol.* **2009**, *373*, 177.

53. Abedi-Koupai, J.; Sohrab, F.; Swarbrick, G. *J. Plant. Nutr.* **2008**, *31*, 317.

54. Sivapalan, S. *Aust. J. Exp. Agr.* **2006**, *46*, 579.

55. Lentz, R. D. and Sojka, R. E. *Agron. J.* **2009**, *101*, 305–314.

56. Taban, M.; Naeini, S. A. R. M. *Commun. Soil Sci. Plant. Anal.* **2006**, *37*, 2031.

57. Bhardwaj, A. K.; McLaughlin, R. A.; Shainberg, I.; Levy, G. J. *Soil Sci. Soc. Am. J.* **2009**, *73*, 910.

58. Al-Harbi, A. R.; Al-Omran, A. M.; Shalaby, A. A.; Choudhary, M. I. *Hort. Sci.* **1999**, *34*, 223–224.